Polymer Chemistry

Accepted Manuscript

ROYAL SOCIETY OF CHEMISTRY

www.rsc.org/polymers

Polymer Chemistry

Dynamic Article Links ►

Cite this: DOI: 10.1039/c0xx00000x

www.rsc.org/xxxxxx

PAPER

A New High Conjugated Crossed Benzodithiophene and Its Donor-Acceptor Copolymers for High Open Circuit Voltages Polymer Solar Cells

Deyu Liu [‡,a,b], Chunyang Gu [‡,b], Manjun Xiao [b], Meng Qiu [b], Mingliang Sun [a*], Renqiang Yang [b*]

Received (in XXX, XXX) Xth XXXXXXXXX 20XX, Accepted Xth XXXXXXXXX 20XX
DOI: 10.1039/b000000x

A novel benzodithiophene-substituted benzodithiophene (crossed-BDT) with enlarged conjugated skeleton was designed and synthesized as an electron-rich unit for constructing donor-acceptor copolymers. Different acceptors, including 4,7-di(thiophen-2-yl)-2,1,3-benzothiadiazole (DTBT) and 4,7-di(thiophen-2-yl)-5,6-difluoro-2,1,3-benzothiadiazole (DTffBT) were used as electron-deficient units for the target copolymers to investigate the effect of inclusion of two fluorine atoms on the acceptor unit of the polymer. Crossed-BDT and DTBT based polymer show high open circuit voltages (V_{oc}) of over 0.9 V with decent power conversion efficiency (PCE) of 3.74%. Crossed-BDT and DTffBT based polymer show nearly 1 V (0.95 V) V_{oc} due to the fluorine induced low-lying HOMO energy level. The 0.9-0.95 V is an impressive V_{oc} result for one 1.7 eV band gap (E_g) polymer. To the best of our knowledge, this is the first report about crossed conjugated benzodithiophene building block design, and this building block is effective to improve V_{oc} for low band gap DBT polymer.

1. Introduction

Recently there is increasing interest in the development of polymer solar cells (PSCs) due to the potential for the fabrication of light-weight, large-area, and flexible light-harvesting devices through low-cost solution processing.[1-5] In recent years, tremendous progress has been made in PSCs field, and the power conversion efficiency (PCE) of PSCs have exceeded 10%.[6] One of the key components of PSCs is the active layer, which determines the solar light harvest and the open-circuit voltage (V_{oc}) of the device. Since fullerenes possess excellent isotropic electron-transporting properties and a low-lying lowest unoccupied molecular orbital (LUMO) level that facilitates exciton separation, they have been frequently used as electron acceptors in PSCs.[7-11] Therefore, new donor polymers should be designed to match the LUMO energy levels of the fullerene derivatives.[12-16] In this regard, donor-acceptor (D-A) copolymers are widely designed and synthesized due to their low band gaps and efficient optical absorption.[17,18] However, the acceptor units, generally introduced in D-A copolymers, will influence the highest occupied molecular orbital (HOMO) level obviously, and then influence the V_{oc} of the PSCs devices. Therefore, researchers concentrate on the design and synthesis of materials with low-lying HOMO level. For some reported high efficient materials, which don't exhibit very low-lying HOMO levels, researchers could use many methods to optimize their short circuit current density (J_{sc}), including using the additive DIO[3,13] and thermal treatment,[19,20] and etc. However, there is relatively less method to improve the V_{oc} of PSCs based on this kind of donor materials.

Among the reported efficient low band gap polymers, the benzodithiophene (BDT) based copolymers have attracted interest as electron donors in the PSCs field due to its rigidity, coplanarity by fusing a benzene with two flanking thiophene units, high hole mobility and high conjugated structures.[21-24] Recently, many BDT copolymers with different conjugated units showed promising photovoltaic properties, with high PCEs of more than 8%.[25-28] As structural modifications on BDT, two dimensional (2-D) conjugated structures have been used to enhance intermolecular π-π interactions, which can be beneficial in improving the photovoltaic properties of conjugated polymers.[29-33] Such as, replacement of the alkoxy moiety by an alkylthienyl has been used to improve the photovoltaic properties of BDT-based polymers.[31,32] However, some well-known efficient BDT-based polymers didn't exhibit high enough V_{oc}, such as the polymers using BDT as the donor units and 4,7-di(thiophen-2-yl)-2,1,3-benzothiadiazole (DTBT) as the acceptor units, which show 0.6-0.82 V V_{oc}.[34-39] As we know, attaching fluorine (F) atoms to the conjugated backbone is one available approach to improve the V_{oc}. As a result, the V_{oc} of the polymers could be improved (0.76-0.90 V).[40-42] In addition, introducing the large side groups into BDT unit was another strategy to improve the V_{oc}.[43,44] In the middle of 2012, Stefan et al. reported the bithiophene-substituted BDT unit with extended conjugated side groups, which could be used as donor and exhibited a high V_{oc} around 1 V.[44] Recently, our group also considered this strategy to improve the V_{oc}, which could make V_{oc} up to 0.8-0.91 V in the BDT and DTBT backboned polymer.[45-47] In summary, with years of efforts, the polymers based on BDT donor unit and DTBT acceptor unit show finally the 0.6-0.91 V V_{oc}.

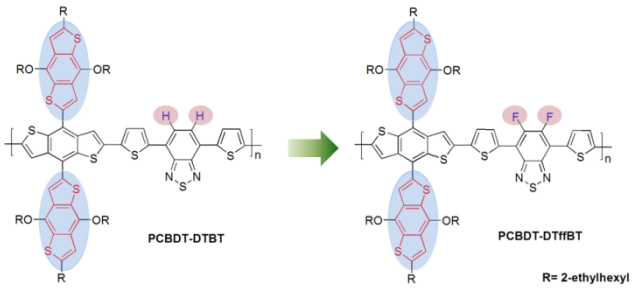

Scheme 1. Molecular Structures of PCBDT-DTBT and PCBDT-DTffBT

In this work, we designed and synthesized a novel benzodithiophene-substituted benzodithiophene (crossed-BDT) as a donor building block for D-A low band gap DBT polymers. Two crossed-BDT based copolymers (see Scheme 1) with two different acceptor units, 4,7-di(thiophen-2-yl)-2,1,3-benzothiadiazole (DTBT) and 4,7-di(thiophen-2-yl)-5,6-difluoro-2,1,3-benzothiadiazole (DTffBT), were synthesized by Stille polycondensation. As a result, the polymers show the V_{oc} of 0.9-0.95 V, which was very high in the same backbone polymers reported in literatures, while PCE of polymers were decent relatively. Thus, we believe that the crossed-BDT building block is an excellent donor unit which could availably improve the V_{oc} of BDT-based polymers with low band gap and high efficiency. This will help researchers to design more efficient novel BDT materials with low band gap and high V_{oc}.

2. Results and discussion

2.1. Synthesis of monomers and polymers

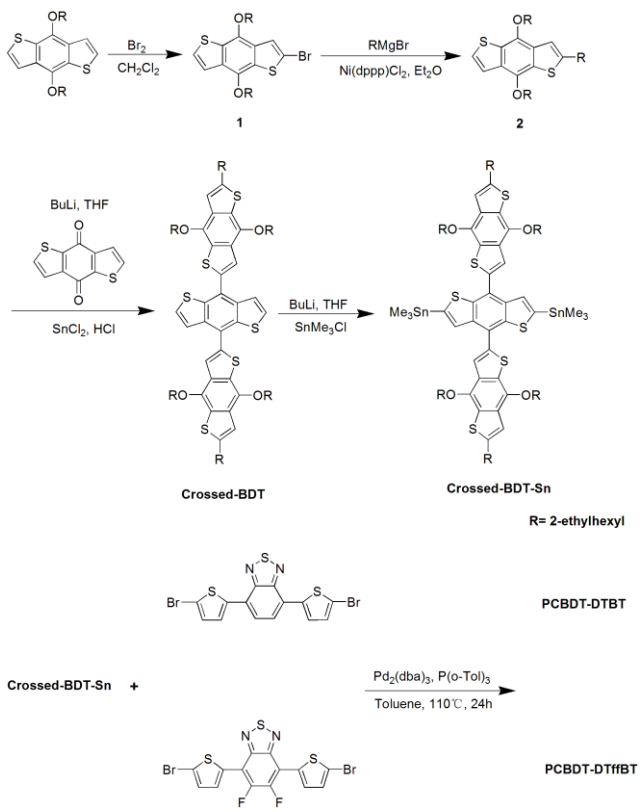

Scheme 2. Synthetic routes of the crossed-BDT monomer and the polymers

Table 1 Molecular weights and thermal properties of PCBDT-DTBT and PCBDT-DTffBT

Polymers	M_n	M_w	PDI	T_d(℃)
PCBDT-DTBT	22.9 K	54.2 K	2.36	336
PCBDT-DTffBT	26.5 K	35.0 K	1.32	338

The synthetic routes of crossed-BDT monomer and corresponding polymers are outlined in Scheme 2. The key intermediate, 2-ethylhexyl-4,8-bis[(2-ethylhexyl)oxy]benzo[1,2-*b*:4,5-*b*']dithiophene (2), was prepared using Grignard reagent, which show higher yield than the n-BuLi based method. This is also the first example demonstrating that alkyl chain can be successfully connected to the 2-position of BDT unit. The copolymers were obtained through Stille-coupling polymerization using $Pd_2(dba)_3$ and P(o-tol)$_3$ as catalysts. The structures of the copolymers were confirmed by ^{1}H NMR spectroscopy. The two copolymers were dissolved in hot chloroform. The number-average molecular weight (M_n) and polydispersity index (PDI) were measured by gel permeation chromatography (GPC) using THF as the eluant and polystyrenes as the internal standards, and the results were listed in Table 1. The M_n of PCBDT-DTBT and PCBDT-DTffBT are 22.9 K and 26.5 K, respectively.

2.2. Thermal analysis

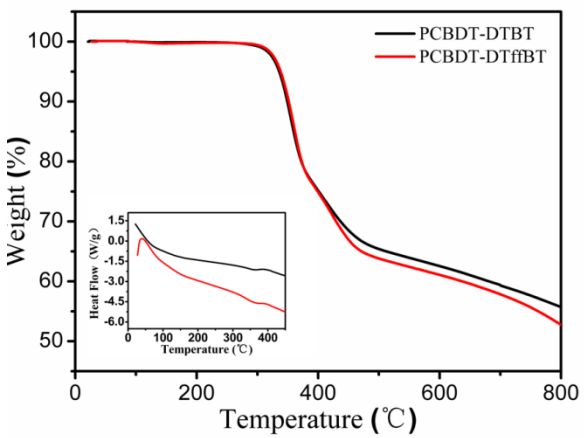

Fig. 1 TGA of the polymers with a heating rate of 10 ℃/min under an inert atmosphere (Inset: DSC thermogram of polymers).

The thermal properties of the polymers were determined by differential scanning calorimetry (DSC) and thermogravimetric analysis (TGA), as shown Fig. 1. DSC thermogram didn't show obvious glass transitions for PCBDT-DTBT and PCBDT-DTffBT polymer under test conditions. The TGA analysis reveals that the onset temperature with 5% weight-loss (T_d) of PCBDT-DTBT and PCBDT-DTffBT are 336 ℃ and 338 ℃, respectively. This indicates that the thermal stability of the polymers is good enough for PSCs applications.

2.3. Optical properties

Table 2 Optical properties and energy levels of the polymers

Polymers	λ_{max} solution (nm)	λ_{max} film (nm)	E_g^{opt} film (eV)	$HOMO^{cv}$ (eV)	$LUMO^{cv}$ (eV)	E_g^{cv} (eV)	$HOMO^{DFT}$ (eV)	$LUMO^{DFT}$ (eV)	E_g^{DFT} (eV)
PCBDT-DTBT	627	640	1.69	-5.26	-3.53	1.73	-5.00	-2.75	2.25
PCBDT-DTffBT	612	624	1.77	-5.34	-3.60	1.74	-5.07	-2.84	2.23

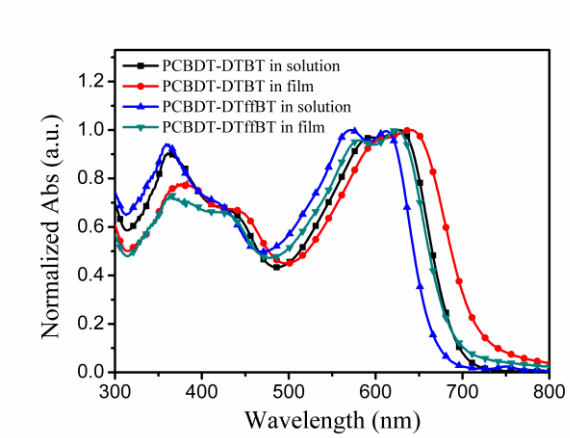

Fig. 2 Normalized absorption spectra of PCBDT-DTBT and PCBDT-DTffBT in chloroform solution and in thin film.

The UV-vis absorption spectra of PCBDT-DTBT and PCBDT-DTffBT in chloroform solution and in thin film are shown in Fig. 2, respectively, and the corresponding absorption properties are summarized in Table 2. Both polymers display relatively similar absorption curves with two absorption bands observed commonly from D-A conjugated copolymers. A π-π* transition feature is observed at around 360 nm. And the main absorption peaks are located at about 627 nm and 612 nm in chloroform solution for PCBDT-DTBT and PCBDT-DTffBT, respectively, which are attributed to the intramolecular charge transfer interaction in D-A systems. However, in the thin film, the absorption spectra peaked at about 640 and 624 nm for PCBDT-DTBT and PCBDT-DTffBT, respectively. Both polymers exhibit a red-shift in the absorption maximum and onset, which is attributed to solid state packing effects, planarizing the polymer backbone. The optical band gaps (E_g^{opt}) of PCBDT-DTBT and PCBDT-DTffBT were estimated to be 1.69 eV and 1.77 eV according to $E_g^{opt}=1240/\lambda$.

2.4. Electrochemical properties

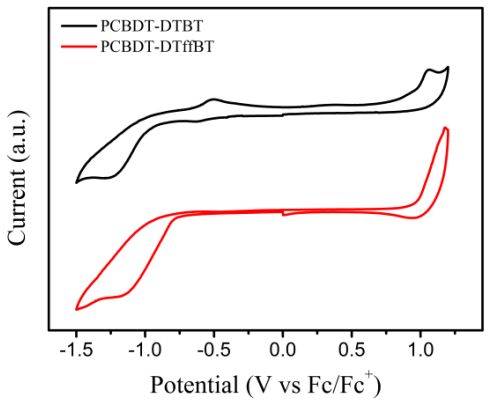

Fig. 3 Cyclic voltammogram of PCBDT-DTBT and PCBDT-DTffBT.

The electrochemical cyclic voltammetry (CV) was performed for determining the highest occupied molecular orbital (HOMO) and the lowest unoccupied molecular orbital (LUMO) energy levels of the conjugated polymers.[48] Fig. 3 shows the cyclic voltammogram (CV) properties of the polymers. A three electrode cell consisting of a glassy carbon working electrode, a platinum wire counter electrode and a saturated calomel reference electrode has been used. The potentials were internally calibrated using the Fc/Fc^+ redox couple. The redox potential of the Fc/Fc^+ internal reference is found to be 0.43 V vs. SCE. According to the empirical equation,

$$HOMO = -(E_{ox}+4.4)\ (eV)$$
$$LUMO = -(E_{re}+4.4)\ (eV)$$

The results of the electrochemical properties are listed in Table 2.The HOMO and LUMO levels of PCBDT-DTBT and PCBDT-DTffBT were -5.26 eV and -3.53 eV, and -5.34 eV and -3.60 eV, respectively. The LUMO energy levels are higher than that of the $PC_{61}BM$ acceptor (-3.9 eV) to ensure energetically favorable electron transfer. It should be noted that the HOMO energy of fluorinated polymer PCBDT-DTffBT (-5.34 eV) is lower than that of the corresponding nonfluorinated polymer PCBDT-DTBT (-5.26 eV) due to the two electron-withdrawing fluorine atoms on the BT units. These two polymers show deep HOMO energy levels (~-5.3 eV), which is desirable for good stability in the air and high open circuit voltage (V_{oc}) in PSCs. The electrochemical band gaps (E_g^{cv}) were also calculated to be 1.73 eV and 1.74 eV for PCBDT-DTBT and PCBDT-DTffBT, respectively, which agree well with the E_g^{opt}. (See Table 2)

2.5. Quantum mechanical calculations

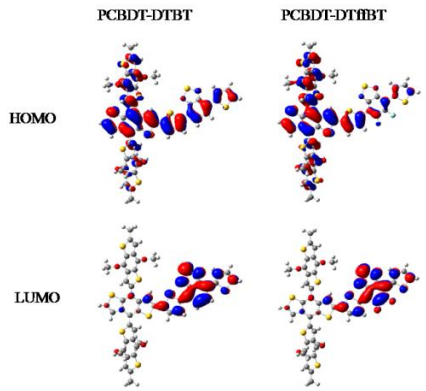

Fig. 4 The HOMO and LUMO surfaces of PCBDT-DTBT and PCBDT-DTffBT

The electron density of states distribution of these two polymers was calculated using density functional theory (DFT) method. All DFT calculations were performed using Gaussian 09 (A.02) employing the hybrid B3LYP exchange-correlation functional with a split valence 6-31G* basis set. One repeating D-A units as illustrated in Fig. 4 were used for computational simplicity. The 2-ethylhexyl side chains were also truncated to methyl groups as their replacement with shorter chains can effectively reduce the calculation time. Both polymers have a delocalized HOMO that is equally distributed over both the donor and acceptor parts of the molecule. However, the LUMO is significantly more localized on the acceptors units. The calculated HOMO and LUMO energy levels are depicted in Table 2. Both the LUMO and HOMO energy levels of PCBDT-DTffBT were slightly lower than those of PCBDT-DTBT. The simulated data from the DFT calculations was generally in agreement with the experimental results estimated from the cyclic voltammograms.

2.6. Photovoltaic properties

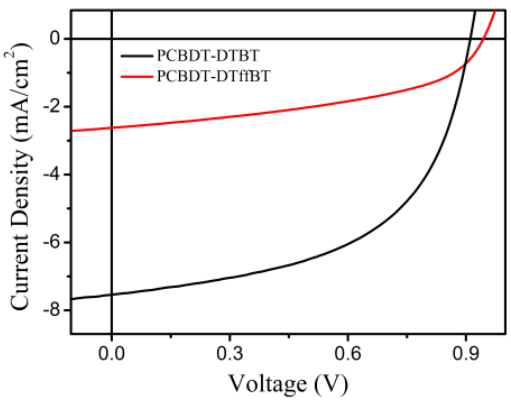

Fig. 5 *J-V* curves of the PSCs based on the blend of PCBDT-DTBT or PCBDT-DTffBT/$PC_{61}BM$ under the illumination of AM 1.5G, 100mWcm^{-2}

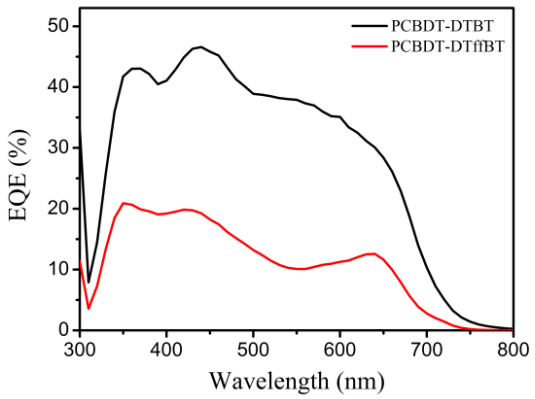

Fig. 6 EQE of curves of the PSCs based on the blend of PCBDT-DTBT or PCBDT-DTffBT/$PC_{61}BM$

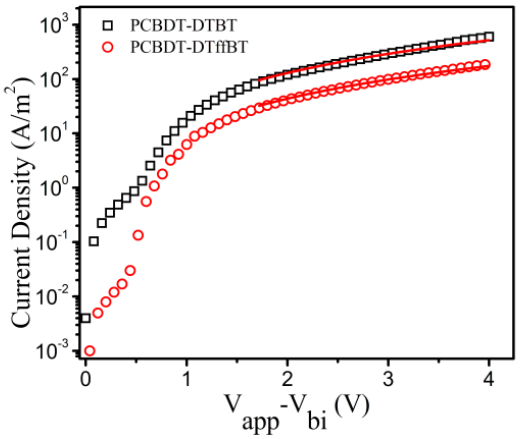

Fig. 7 Current density (*J*)-voltage (*V*) curves for PCBDT-DTBT and PCBDT-DTffBT based devices (the symbols are experimental data for transport of hole, and the red lines are fitted according to the space-charge-limited-current model).

Table 3 PSCs devices performance of PCBDT-DTBT or PCBDT-DTffBT

Polymers/ Acceptor	D/A	V_{oc} (V)	J_{sc} (mAcm^{-2})	FF (%)	PCE_{max} (PCE_{ave})[a] (%)
PCBDT-DTBT/$PC_{61}BM$	1:1	0.91	6.12	41.74	2.32 (2.09)
PCBDT-DTBT/$PC_{61}BM$	1:2	0.91	7.54	54.56	3.74[b] (3.45)
PCBDT-DTBT/$PC_{61}BM$	1:3	0.91	6.19	58.24	3.28 (3.06)
PCBDT-DTBT/$PC_{71}BM$	1:2	0.90	4.80	52.11	2.25 (2.09)
PCBDT-DTffBT/$PC_{61}BM$	1:1	0.95	2.35	43.41	0.97 (0.87)
PCBDT-DTffBT/$PC_{61}BM$	1:2	0.94	2.62	46.13	1.14[c] (1.08)
PCBDT-DTffBT/$PC_{61}BM$	1:3	0.93	2.51	42.38	0.99 (0.83)
PCBDT-DTffBT/$PC_{71}BM$	1:2	0.94	2.35	51.05	1.13 (0.98)

[a] The average PCE is obtained from 5 devices.
[b,c] The active layer blend film thickness are 115 nm and 110 nm, respectively.

Table 4 Comparison photovoltaic properties of PSCs devices of PCBDT-DTBT and PCBDT-DTffBT with analogs

Polymers (D)	Acceptors (A)	D:A (w:w)	E_g (eV)	V_{oc} (V)	E_g-eV_{oc} (eV)	J_{sc} (mAcm^{-2})	FF (%)	PCE_{max} (PCE_{ave}) (%)	Ref.
PCBDT-DTBT	$PC_{61}BM$	1:2	1.69	0.91	0.78	7.54	54.56	3.74 (3.45)	This work
$PBDT_{ODO}$-DTBT	$PC_{71}BM$	1:1	1.72	0.72	1.00	11.16	62	5.01 (4.90)	36
$PBDT_{THO}$-DTBT	$PC_{71}BM$	1:2	1.70	0.68	1.02	8.45	56.5	3.24 (3.10)	39
PCBDT-DTffBT	$PC_{61}BM$	1:1	1.77	0.95	0.82	2.35	43.41	0.97 (0.87)	This work
PCBDT-DTffBT	$PC_{61}BM$	1:2	1.77	0.94	0.83	2.62	46.13	1.14 (1.08)	This work
$PBDT_{BN}$-DT_{EH}ffBT	$PC_{61}BM$	1:1	1.73	0.90	0.83	12.2	62.1	7.16 (6.64)	40
$PBDT_{TEH}$-DT_{EH}ffBT	$PC_{71}BM$	1:1.5	1.76	0.76	1.00	13.17	61.9	6.20 (6.03)	42

Bulk heterojunction PSCs devices with a configuration of ITO/PEDOT:PSS/polymers:$PC_{61}BM$/Ca/Al were fabricated by the method of solution processing as our previous work.[49-51] Current density versus voltage (*J-V*) curves of the PSCs based on PCBDT-DTBT and PCBDT-DTffBT under illumination of AM 1.5G, 100 mWcm^{-2} were shown in Fig. 5. Due to the limited solubility, these two polymers blended with the acceptor $PC_{61}BM$ in chloroform solution were heated at 90 ℃ for 2 h before spin-coated as the active layer. The weight ratios of PCBDT-DTBT and PBDT-DTffBT to $PC_{61}BM$ varied from 1:1 to 1:3 for device optimization. Table 3 summarized the detailed device performances. A blend ratio of 1:2 was found to give the best results for both polymers. $PC_{71}BM$ were also used as acceptor with the device configuration ITO/PEDOT:PSS/polymers:$PC_{71}BM$ (1:2)/Ca/Al to optimize devices performances. However, photovoltaic properties of the devices weren't improved. Finally, the best solar cells based on PCBDT-DTBT showed a PCE of 3.74% with an V_{oc} of 0.91 V, a J_{sc} of 7.54 mAcm^{-2}, and a FF of 54.56% and PCBDT-DTffBT showed a PCE of 1.14% with an V_{oc} of 0.94 V, a J_{sc} of 2.62 mAcm^{-2}, and a FF of 46.13% at the same condition. It was interestedly noted that these two polymers show high V_{oc} PSCs devices due to their lower-lying HOMO energy level, which agree well with our expectations. Side substituted groups could affect the V_{oc} of the polymer solar cells. Especially, bulky conjugated side group will lower the HOMO levels of polymers to improve the V_{oc}, as the V_{oc} is related to the energy difference between the HOMO of polymer and the LUMO of acceptor.[43,44] Unfortunately, the PCEs of two polymers were moderate, which was attributed to their poor solubility. What's more, the large side groups connected to the crossed-BDT units could affect the intermolecular packing to cause the low J_{sc}. This could be another reason for the unsatisfactory PCEs. On the other hand, compared to PCBDT-DTBT, PBDT-DTffBT showed a increased V_{oc} by fluorination, which was in conformity with previous reports.[40-42]

For polymer PCBDT-DTBT and PCBDT-DTffBT, the detailed photovoltaic performances are compared with these of the polymers which have the same backbone structure but do not have the bulky BDT side group ($PBDT_{ODO}$-DTBT,[36] $PBDT_{THO}$-DTBT,[39] $PBDT_{BN}$-DT_{EH}ffBT [40] and $PBDT_{TEH}$-DT_{EH}ffBT [42]). The detailed optical-electronic properties and PSCs devices performances are listed in Table 4. As a result, our bulky BDT side group does help for high V_{oc}. The PCBDT-DTBT show higher V_{oc} than those of $PBDT_{ODO}$-DTBT with typically 1-D alkoxy side chain and $PBDT_{THO}$-DTBT with typically 2-D alkylthienyl side group, by 26% and 34%, respectively. Similarly, compared with 1-D $PBDT_{BN}$-DT_{EH}ffBT and 2-D $PBDT_{TEH}$-DT_{EH}ffBT, the PCBDT-DTffBT also show higher V_{oc}. To highlight the high V_{oc} feature of devices, researchers define the donor photon energy loss as E_g-eV_{oc}, where E_g is the optical band gap of the donor polymer and V_{oc} is obtained from the corresponding device with either $PC_{61}BM$ or $PC_{71}BM$.[51] As shown in Table 4, the PCBDT-DTBT show almost the same E_g with $PBDT_{ODO}$-DTBT and $PBDT_{THO}$-DTBT, but much lower E_g-eV_{oc}. Compared with $PBDT_{BN}$-DT_{EH}ffBT, the PCBDT-DTffBT show the similar E_g and E_g-eV_{oc}, but much lower E_g-eV_{oc} than $PBDT_{TEH}$-DT_{EH}ffBT. In conclusion, the bulky BDT side group helps to improve V_{oc} of the PSCs devices.

To verify the accuracy of the *J-V* measurements, the corresponding external quantum efficiency (EQE) of the devices were measured and shown in Fig. 6. Both polymers exhibited broadened absorption from 350-800 nm. The EQE value of PCBDT-DTBT is higher than that of PCBDT-DTffBT in whole parts of spectra and the maximum value reaches 46%. It indicates that PCBDT-DTBT has a much better photo response among the absorption range. The calculated current density from the EQE measurement were 7.22 mAcm^{-2} and 2.56 mAcm^{-2}, respectively for PCBDT-DTBT and PCBDT-DTffBT, which agree well with the J_{sc} (7.54 mAcm^{-2} for PCBDT-DTBT and 2.62 mAcm^{-2} for PCBDT-DTffBT) obtained from the *J-V* measurements.

In addition to the absorption and energy levels, charge carrier mobility is another crucial factor for achieving high-efficiency devices. The hole mobilities of the two polymers were measured via space charge limited current (SCLC) method,[53] with the

device structure of ITO/PEDOT:PSS/polymers:$PC_{61}BM$/Au. As shown in Fig. 7, the hole mobilities are calculated to be 1.68×10^{-5} $cm^2V^{-1}s^{-1}$ and 4.93×10^{-6} $cm^2V^{-1}s^{-1}$ for PCBDT-DTBT and PCBDT-DTffBT, respectively. The SCLC results show that the hole mobility of PCBDT-DTBT is higher than that of PCBDT-DTffBT. This could be a potential reason that PCBDT-DTBT:$PC_{61}BM$ based devices exhibit larger J_{sc} and FF than PCBDT-DTffBT:$PC_{61}BM$ based device.

2.7. Morphological Characterization

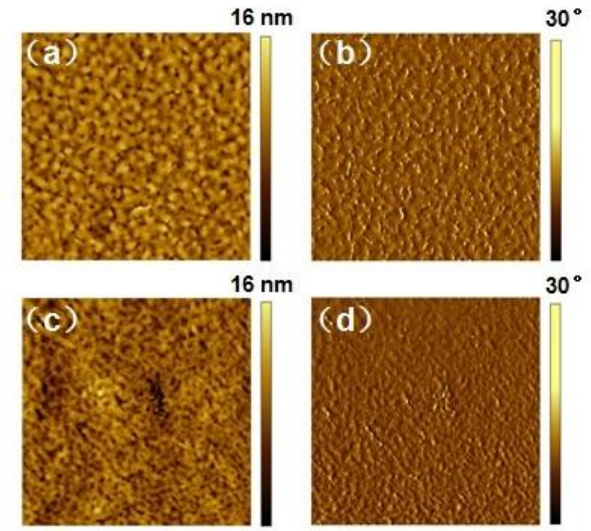

Fig. 8 AFM height (a) and phase (b) images of the PCBDT-DTBT:$PC_{61}BM$ (1:2) blend films; AFM height (c) and phase (d) images of the PCBDT-DTffBT:$PC_{61}BM$ (1:2) blend films. All the images are 5 μm×5 μm.

Atomic force microscopy (AFM) was used to investigate the morphology of the two polymers: $PC_{61}BM$ blend films. The height images and phase images of the blends are shown in Fig. 8. The root-mean-square (RMS) of the PCBDT-DTBT and $PC_{61}BM$ blend films was 1.84 nm. Compared with PCBDT-DTBT, the blend films of PCBDT-DTffBT and $PC_{61}BM$ showed a lower surface roughness with RMS of 0.78 nm, which indicated that PCBDT-DTffBT showed better compatibility with $PC_{61}BM$.

3. Conclusions

In summary, we have successfully designed and synthesized a novel highly-conjugated crossed benzodithiophene (crossed-BDT) as an electron-rich unit for constructing two donor-acceptor copolymers. The BT unit, as acceptor, was also modified with unfluorine and fluorine moieties. A decrease in the HOMO level and a net blue-shifted absorption of the fluorinated polymer compared with the unfluorinated polymer is observed. These two copolymers with crossed-BDT structure in the backbone showed the desired deep HOMO energy levels. The crossed-BDT donor can availably improve the V_{oc} of polymers with DTBT backbone, which show 0.9-0.95 V V_{oc}. Therefore, this will provide some reference to improve the V_{oc} of low band gap BDT materials based PSCs device. To improve the PCE, further work of making long branched alkyl substituted polymer with the same backbone is underway.

4. Experimental

4.1. Materials

All starting reagents were obtained commercially as analytical reagent and used directly without any purification. Toluene, ether and THF were purified by vacuum distillation under nitrogen prior to use. 4,8-Bis[(2-ethylhexyl)oxy]benzo[1,2-*b*:4,5-*b*'] dithiophene, 4,7-bis(5-bromo-2-thienyl)-2,1,3-benzothiadiazole and 4,7-bis(5-bromo-2-thienyl)-5,6-difluoro-2,1,3-benzothiadiazole were synthesized as reported in the literature.[54-56]

4.2. Instruments and measurements

Nuclear magnetic resonance (NMR) spectra were taken on a Bruker AVANCE-III 600 Spectrometer. High resolution mass spectra (MS) were recorded under APCI mode on a Bruker Maxis UHRTOF spectrometer. Differential scanning calorimetry (DSC) and thermal gravimetric analysis (TGA) measurements were performed on STA-409 at a heating rate of 10 ℃min^{-1}. UV-Vis absorption spectrum was measured with a Hitachi U-4100 spectrophotometer. The polymer films on quartz used for absorption spectral measurement were prepared by spin-coating from their chloroform solutions. Cyclic voltammetry (CV) was performed using a CHI660D electrochemical workstation with a glassy carbon working electrode, a saturated calomel reference electrode (SCE) and a platinum wire counter electrode at a scan rate of 100 mVs^{-1}. Tetrabutylammonium phosphorus hexafluoride (Bu_4NPF_6, 0.1 M) in acetonitrile was used as the supporting electrolyte. Surface morphological characterizations of the films were characterized by a tapping-mode atomic force microscope (AFM, Agilent 5400). X-ray diffraction (XRD) pattern were recorded on a Bruker D8 Advance.

4.3. Fabrication and characterization of polymer solar cells

Photovoltaic devices were fabricated on pre-patterned indium tin oxide (ITO) coated glass substrates with a layered structure of ITO/PEDOT:PSS/donor:acceptor/Ca(10 nm)/Al(100 nm). The ITO coated glass substrates were cleaned in ultrasonic bath in acetone, toluene, methanol and isopropyl alcohol sequentially. And then, oxygen plasma treatment was made for 20 min, spin-coated with PEDOT:PSS at 5000 rpm, and dried under argon for 20 min at 120 ℃. Subsequently, the active layer was spin-coated from different blend weight ratios of donor (12 mg/ml) and $PC_{61}BM$ in deoxygenated anhydrous chloroform solution on the ITO/PEDOT:PSS substrate. The active layer thickness was about 100 nm, measured by a Dektak 150 profilometer. Finally, Ca (10 nm) and aluminum (100 nm) were thermally evaporated at a vacuum of ~2×10^{-4} Pa on top of active layer. The active area of the solar cell devices was 0.1 cm^2. The current density-voltage (*J-V*) characteristics were measured with a Keithley 2420 source measurement unit under simulated 100 $mWcm^{-2}$ (AM 1.5 G) irradiation from a Newport solar simulator. Light intensity was calibrated with a standard silicon solar cell. The external quantum efficiencies (EQE) of solar cells were analyzed using a certified Newport incident photon conversion efficiency (IPCE) measurement system.

4.4. Synthesis

Synthesis of 2-bromo-4,8-bis[(2-ethylhexyl)oxy]benzo[1,2-b:4,5-b']dithiophene (1)

In a 500 ml flask, 4,8-bis[(2-ethylhexyl)oxy]benzo[1,2-b:4,5-b']dithiophene (17.87 g, 40 mmol) was dissolved in dichloromethane (200 ml). Bromine (6.39 g, 40 mmol) was dissolved into dichloromethane (80 ml) in a funnel and slowly dropped into the flask under an ice-water bath. After stirring under dark at room temperature for 3.5 h, the solvent was removed under vacuum and residue was purified by silica column chromatography with petroleum ether/ dichloromethane (8/1, v/v) to give compound **1** as a pale yellow oil (9.04 g, 43%). ^{1}H NMR (600 MHz, $CDCl_3$): δ (ppm) 7.43 (s, 1H), 7.41 (d, J=5.4 Hz, 1H), 7.33 (d, J=5.4 Hz, 1H), 4.14-4.07 (m, 4H), 1.80-1.72 (m, 2H), 1.69-1.33 (m, 16H), 1.02-0.97 (m, 6H), 0.96-0.91 (m, 6H).

Synthesis of 2-ethylhexyl-4,8-bis[(2-ethylhexyl)oxy]benzo[1,2-b:4,5-b']dithiophene (2)

A stirred mixture of Mg (1.31 g, 54 mmol) and I_2 (0.13 g, 0.5 mmol) in 25 mL of anhydrous diethyl ether was heated to reflux for 3 min under argon, and then 2-ethylhexyl bromide (9.27 g, 48 mmol) in anhydrous diethyl ether (35 ml) was added dropwise. The solution was refluxed for 3 h and cooled to room temperature. The prepared 2-ethylhexylmagnesium bromide solution was added dropwise to an ice-cooled and stirring mixture of compound 1 (8.41 g, 16 mmol) and Ni(dppp)Cl_2 (0.087 g, 0.16 mmol) in anhydrous diethyl ether (80 ml). The cooling bath was removed and the mixture was heated to reflux, stirred overnight and quenched with ammonium chloride saturated solution (60 mL). The organic and inorganic parts were separated and the aqueous part was extracted with diethyl ether. The combined organic parts were washed with water and dried over anhydrous Na_2SO_4. The solvent was removed under vacuum and residue was purified by silica column chromatography with petroleum ether/ dichloromethane (10/1, v/v) to give compound **2** as a clear oil (2.86 g, 32%).^{1}H NMR (600 MHz, $CDCl_3$): δ (ppm) 7.44 (d, J=5.4 Hz, 1H), 7.31 (d, J=5.4 Hz, 1H), 7.10 (s, 1H), 4.18-4.11 (m, 4H), 2.84 (d, J=7.2 Hz, 2H), 1.82-1.76 (m, 2H), 1.74-1.25 (m, 25H), 1.03-0.99 (m, 6H), 0.96-0.83 (m, 12H).

Synthesis of Crossed-BDT

To a solution of compound 2 (2.63 g, 4.7 mmol) in THF (15 ml) at 0 ℃ under argon, n-BuLi (3.62 ml, 5.8 mmol, 1.6 M in hexane) was added dropwise. The reactant mixture was heated up to 50 ℃ for 2 h. After that, 4,8-dehydrobenzo[1,2-b:4,5-b']dithiophene-4,8-dione (0.44 g, 2 mmol) was added, and the mixture was kept at 50 ℃ for 3 h. Cooling the mixture down to room temperature, $SnCl_2$ $2H_2O$ (3.61 g, 16 mmol) in 8 ml HCl (10%) was added, and the mixture was stirred for another 3 h. The mixture was poured into ice water and extracted by petroleum ether. The combined extracts were dried over anhydrous Na_2SO_4. The solvent was removed under vacuum and residue was purified by silica column chromatography with petroleum ether/ dichloromethane (8/1, v/v) to give crossed-BDT as a yellow solid (1.46 g, 56%). ^{1}H NMR (600 MHz, $CDCl_3$): δ (ppm) 7.86 (s, 2H), 7.77 (d, J=6.0, 2H), 7.54 (d, J=5.4, 2H), 7.16 (s, 2H), 4.27-4.20 (m, 8H), 2.88 (d, J=6.6 Hz, 4H), 1.85-1.79 (m, 4H), 1.76-1.27 (m, 50H), 1.04-0.98 (m, 12H), 0.97-0.86 (m, 24H).

Synthesis of Crossed-BDT-Sn

To a solution of crossed-BDT (1.30 g, 1 mmol) in THF (25 ml) at 0 ℃, n-BuLi (1.56 ml, 2.5 mmol, 1.6 M in hexane) was added dropwise. The mixture was stirred at 0 ℃ for 30 min and then warm to 50 ℃ for 1.5 h. After cooling back to 0 ℃ again, trimethyltin chloride (3 ml, 1 M in hexane) was added dropwise. The mixture was brought to room temperature and stirred overnight. Water was subsequently added to the reaction mixture and the organic component was extracted by diethyl ether. The combined organic extracts were dried over Na_2SO_4 and the solvent was removed under reduced pressure. The residue was recrystallized by isopropyl alcohol one time. Crossed-BDT-Sn was obtained as a yellow solid (0.95 g, 58%). ^{1}H NMR (600 MHz, $CDCl_3$): δ (ppm) 7.88 (s, 2H), 7.82 (s, 2H), 7.15 (s, 2H), 4.27-4.20 (m, 8H), 2.88 (d, J=6.6 Hz, 4H), 1.85-1.79 (m, 4H), 1.76-1.27 (m, 50H), 1.04-0.98 (m, 12H), 0.97-0.86 (m, 24H), 0.39 (s, 18H). ^{13}C NMR (151 MHz, $CDCl_3$): δ (ppm) 145.69, 144.54, 143.66, 143.45, 143.29, 139.45, 137.52, 132.31, 130.92, 130.83, 130.18, 129.72, 122.65, 121.29, 117.76, 76.27, 75.90, 41.03, 40.67, 40.64, 35.35, 32.48, 30.48, 30.45, 29.19, 28.86, 25.75, 23.88, 23.13, 23.11, 23.02, 14.17, 14.15, 14.12, 11.38, 11.32, 10.88, -8.35. MS (MALDI-TOF)： cacld for $C_{84}H_{126}O_4S_6Sn_2$ $[M]^+$，1629.6112；found：1629.6094.

Synthesis of PCBDT-DTBT

To a 25 ml flask, crossed-BDT-Sn (163.0 mg, 0.1 mmol), 4,7-bis(5-bromo-2-thienyl)-2,1,3-benzothiadiazole (45.8 mg, 0.1 mmol), $Pd_2(dba)_3$ (2.8 mg, 0.003 mmol), and tri(o-tolyl)phosphine (5.5 mg, 0.018 mmol) were added under argon. After the addition of toluene (5 ml), the mixture was heated to 110 ℃ and maintained at the same temperature for 24 h. After cooling to room temperature, the mixture was poured into methanol. The precipitate was collected and filtered into a Soxhelt funnel and extracted by methanol, acetone, and hexane successively. The residue was collected and dried overnight under vacuum with the yield 62% for PCBDT-DTBT as a black solid. ^{1}H NMR (600 MHz, $CDCl_3$): δ (ppm) 8.05-6.75 (m, 12H), 4.29 (br, 8H), 2.99 (br, 4H), 1.90-0.75 (m, 102H).

Synthesis of PCBDT-DTffBT

To a 25 ml flask, crossed-BDT-Sn (163.0 mg, 0.1 mmol), 4,7-bis(5-bromo-2-thienyl)-5,6-difluoro-2,1,3-benzothiadiazole (49.4 mg, 0.1 mmol), $Pd_2(dba)_3$ (2.8 mg, 0.003 mmol), and tri(o-tolyl)phosphine (5.5 mg, 0.018 mmol) were added under argon. After the addition of toluene (5 ml), the mixture was heated to 110 ℃ and maintained at the same temperature for 24 h. After cooling to room temperature, the mixture was poured into methanol. The precipitate was collected and filtered into a Soxhelt funnel and extracted by methanol, acetone, and hexane successively. The residue was collected and dried overnight under vacuum with the yield 65% for PCBDT-DTffBT as a black solid. ^{1}H NMR (600 MHz, $CDCl_3$): δ (ppm) 8.30-6.95 (m, 12H), 4.29 (br, 8H), 2.97 (br, 4H), 1.85-0.75 (m, 102H).

Acknowledgments

The authors gratefully acknowledge financial support from the NSFC (21274134, 21274161, 51173199), New Century Excellent Talents in University (NCET-11-0473).

Notes

[a] *Institute of Material Science and Engineering, Ocean University of China, Qingdao 266100, People's Republic of China. Fax: 86-532-66781927; Tel: 86-532-66781690; E-mail: mlsun@ouc.edu.cn*

[b] *CAS Key Laboratory of Bio-based Materials, Qingdao Institute of Bioenergy and Bioprocess Technology, Chinese Academy of Sciences, Qingdao 266101, People's Republic of China. Fax: 86-532-80662778; Tel: 86-532-80662700; E-mail: yangrq@qibebt.ac.cn*

†Electronic Supplementary Information (ESI) available: XRD pattern,[1]H NMR and [13]C NMR spectra of monomers and polymers. See DOI: 10.1039/b000000x/

‡ These authors contributed equally to this work.

References

.

1. G. Yu, J. Gao, J. C. Hummelen, F. Wudl and A. J. Heeger, *Science*, 1995, **270**, 1789-1791.
2. C. J. Brabec, *Sol. Energy Mater. Sol. Cells*, 2004, **83**, 273-292.
3. M. Zhang, X. Guo, W. Ma, S. Zhang, L. Huo, H. Ade and J. Hou, *Adv. Mater.*, 2014, **26**, 2089-2095.
4. J. Yuan, Z. Zhai, H. Dong, J. Li, Z. Jiang, Y. Li and W. Ma, *Adv. Funct. Mater*, 2013, **23**, 885-892.
5. M. C. Scharber and N. S. Sariciftci, *Progress in polymer science*, 2013, **38**, 1929-1940.
6. J. You, L. Dou, K. Yoshimura, T. Kato, K. Ohya, T. Moriarty, K. Emery, C. C. Chen, J. Gao, G. Li and Y. Yang, *Nat. Commun.*, 2013, **4**, 1446.
7. F. Wudl, *Acc. Chem. Res.*, 1992, **25**, 157-161.
8. M. Lenes, G.-J. A. H. Wetzelaer, F. B. Kooistra, S. C. Veenstra, J. C. Hummelen and P. W. M. Blom, *Adv. Mater.*, 2008, **20**, 2116-2119.
9. R. B. Ross, C. M. Cardona, D. M. Guldi, S. G. Sankaranarayanan, M. O. Reese, N. Kopidakis, J. Peet, B. Walker, G. C. Bazan, E. Van Keuren, B. C. Holloway and M. Drees, *Nat. Mater.*, 2009, **8**, 208-212.
10. Y. Zhang, H.-L. Yip, O. Acton, S. K. Hau, F. Huang and A. K. Y. Jen, *Chem. Mater.*, 2009, **21**, 2598-2600.
11. Y. He, H.-Y. Chen, J. Hou, Y. Li, Y. Cao, J. Gao, D. Wang, G. Yu and A. J. Heeger, *J. Am. Chem. Soc.*, 2010, **132**, 1377-1382.
12. M. Yuan, P. Yang, M. M. Durban and C. K. Luscombe, *Macromolecules*, 2012, **45**, 5934-5940.
13. Y. Liang, Z. Xu, J. Xia, S. T. Tsai, Y. Wu, G. Li, C. Ray and L. Yu, *Adv. Mater.*, 2010, **22**, E135-E138.
14. J. Hou, H.-Y. Chen, S. Zhang, R. I. Chen, Y. Yang, Y. Wu and G. Li, *J. Am. Chem. Soc.*, 2009, **131**, 15586-15587.
15. M. Wang, X. Hu, P. Liu, W. Li, X. Gong, F. Huang and Y. Cao, *J. Am. Chem. Soc.*, 2011, **133**, 9638-9641.
16. Z. He, C. Zhang, X. Xu, L. Zhang, L. Huang, J. Chen, H. Wu and Y. Cao, *Adv. Mater.*, 2011, **23**, 3086-3089.
17. W. Li, Q. Li, S. Liu, C. Duan, L. Ying, F. Huang, Y. Cao, *Sci. China Chem.*, 2015, **58**: 257-266.
18. Y. Zhang, J. Zou, H.-L. Yip, K.-S. Chen, D. F. Zeigler, Y. Sun and K. Y. J. Alex, *Chem. Mater.*, 2011, **23**, 2289-2291.
19. J. Liu, H. Choi, J. Y. Kim, C. Bailey, M. Durstock and L. Dai, *Adv. Mater.*, 2012, **24**, 538-542.
20. L.-M. Chen, Z. Hong, G. Li and Y. Yang, *Adv. Mater.*, 2009, **21**, 1434-1449.
21. H. Pan, Y. Li, Y. Wu, P. Liu, B. S. Ong, S. Zhu and G. Xu, *Chem. Mater.*, 2006, **18**, 3237-3241.
22. H. Pan, Y. Wu, Y. Li, P. Liu, B. S. Ong, S. Zhu and G. Xu, *Adv. Funct. Mater*, 2007, **17**, 3574-3579.
23. R. S. Kularatne, H. D. Magurudeniya, P. Sista, M. C. Biewer and M. C. Stefan, *J Polym Sci Part A: Polym Chem*, 2013, **51**, 743-768.
24. P. Sista, M. C. Biewer and M. C. Stefan, *Macromol. Rapid Commun*, 2012, **33**, 9-20.
25. Z. He, C. Zhong, S. Su, M. Xu, H. Wu and Y. Cao, *Nat. Photonics*, 2012, **6**, 591-595.
26. C. Cabanetos, A. El Labban, J. A. Bartelt, J. D. Douglas, W. R. Mateker, J. M. Frechet, M. D. McGehee and P. M. Beaujuge, *J. Am. Chem. Soc.*, 2013, **135**, 4656-4659.
27. M. Zhang, Y. Gu, X. Guo, F. Liu, S. Zhang, L. Huo, T. P. Russell and J. Hou, *Adv. Mater.*, 2013, **25**, 4944-4949.
28. H.-C. Chen, Y.-H. Chen, C.-C. Liu, Y.-C. Chien, S.-W. Chou and P.-T. Chou, *Chem. Mater.*, 2012, **24**, 4766-4772.
29. Y. Huang, X. Guo, F. Liu, L. Huo, Y. Chen, T. P. Russell, C. C. Han, Y. Li and J. Hou, *Adv. Mater.*, 2012, **24**, 3383-3389.
30. X. Li, W. C. Choy, L. Huo, F. Xie, W. E. Sha, B. Ding, X. Guo, Y. Li, J. Hou, J. You and Y. Yang, *Adv. Mater.*, 2012, **24**, 3046-3052.
31. L. Huo, S. Zhang, X. Guo, F. Xu, Y. Li and J. Hou, *Angew. Chem., Int. Ed.* , 2011, **50**, 9697-9702.
32. R. Duan, L. Ye, X. Guo, Y. Huang, P. Wang, S. Zhang, J. Zhang, L. Huo and J. Hou, *Macromolecules*, 2012, **45**, 3032-3038.
33. D. Qian, L. Ye, M. Zhang, Y. Liang, L. Li, Y. Huang, X. Guo, S. Zhang, Z. a. Tan and J. Hou, *Macromolecules*, 2012, **45**, 9611-9617.
34. X. Guo, M. Zhang, L. Huo, F. Xu, Y. Wu and J. Hou, *J. Mater. Chem.* , 2012, **22**, 21024-21031.
35. B. Liu, X. Chen, Y. He, Y. Li, X. Xu, L. Xiao, L. Li and Y. Zou, *J. Mater. Chem. A*, 2013, **1**, 570-577.
36. E. Zhou, J. Cong, K. Hashimoto and K. Tajima, *Macromolecules*, 2013, **46**, 763-768.
37. Y. Li, Y. Chen, X. Liu, Z. Wang, X. Yang, Y. Tu and X. Zhu, *Macromolecules*, 2011, **44**, 6370-6381.
38. Y. Huang, F. Liu, X. Guo, W. Zhang, Y. Gu, J. Zhang, C. C. Han, T. P. Russell and J. Hou, *Adv. Energy Mater.*, 2013, **3**, 930-937.
39. P. Zhou, Z.-G. Zhang, Y. Li, X. Chen and J. Qin, *Chem. Mater.*, 2014, **26**, 3495-3501.
40. A. C. Stuart, J. R. Tumbleston, H. Zhou, W. Li, S. Liu, H. Ade and W. You, *J. Am. Chem. Soc.*, 2013, **135**, 1806-1815.
41. H. Zhou, L. Yang, A. C. Stuart, S. C. Price, S. Liu and W. You, *Angew. Chem., Int. Ed.* , 2011, **50**, 2995-2998.
42. N. Wang, Z. Chen, W. Wei and Z. Jiang, *J. Am. Chem. Soc.*, 2013, **135**, 17060-17068.
43. R. S. Kularatne, F. J. Taenzler, H. D. Magurudeniya, J. Du, J. W. Murphy, E. E. Sheina, B. E. Gnade, M. C. Biewer and M. C. Stefan, *J. Mater. Chem. A*, 2013, **1**, 15535-15543.
44. R. S. Kularatne, P. Sista, H. Q. Nguyen, M. P. Bhatt, M. C. Biewer and M. C. Stefan, *Macromolecules*, 2012, **45**, 7855-7862.
45. Q. Liu, X. Bao, S. Wen, Z. Du, L. Han, D. Zhu, Y. Chen, M. Sun and R. Yang, *Polym. Chem.*, 2014, **5**, 2076-2082.
46. L. Han, X. Bao, T. Hu, Z. Du, W. Chen, D. Zhu, Q. Liu, M. Sun and R. Yang, *Macromol. Rapid Commun.*, 2014, **35**, 1153-1157.
47. J. Wang, M. Xiao, W. Chen, M. Qiu, Z. Du, W. Zhu, S. Wen, N. Wang and R. Yang, *Macromolecules*, 2014, **47**, 7823-7830.
48. Y. Li, Y. Cao, J. Gao, D. Wang, G. Yu and A. J. Heeger, *Synth. Met*, 1999, **99**, 243-248.
49. M. Sun, L. Wang, X. Zhu, B. Du, R. Liu, W. Yang and Y. Cao, *Sol. Energy Mater. Sol. Cells*, 2007, **91**, 1681-1687.
50. T. Hu, L. Han, M. Xiao, X. Bao, T. Wang, M. Sun and R. Yang, *J. Mater. Chem. C*, 2014, **2**, 8047-8053.
51. M. Sun, L. Wang, B. Du, Y. Xiong, R. Liu and Y. Cao, *Synth. Met.*, 2008, **158**, 125-129.
52. M. Wang, H. Wang, T. Yokoyama, X. Liu, Y. Huang, Y. Zhang, T. Q. Nguyen, S. Aramaki and G. C. Bazan, *J. Am. Chem. Soc.*, 2014, **136**, 12576-12579.
53. S. C. Price, A. C. Stuart and W. You, *Macromolecules*, 2010, **43**, 4609-4612.
54. J. Hou, M.-H. Park, S. Zhang, Y. Yao, L.-M. Chen, J.-H. Li and Y. Yang, *Macromolecules*, 2008, **41**, 6012-6018.
55. Q. Hou, Y. Xu, W. Yang, M. Yuan, J. Peng and Y. Cao, *J. Mater. Chem.*, 2002, **12**, 2887-2892.
56. X. Guo, H. Xin, F. S. Kim, A. D. T. Liyanage, S. A. Jenekhe and M. D. Watson, *Macromolecules*, 2011, **44**, 269-277.

